Analyst

ROYAL SOCIETY OF CHEMISTRY

PAPER

View Article Online
View Journal

Cite this: DOI: 10.1039/d0an00205d

A novel solution-gated graphene transistor biosensor for ultrasensitive detection of trinucleotide repeats†

Zhiqi Ge,[a] Mingyu Ma,[b] Gang Chang,[b] Meijun Chen,[a] Hanping He,*[a] Xiuhua Zhang[a] and Shengfu Wang[a]

A new way to detect GAA trinucleotide repeats (TNRs) based on a solution-gated graphene transistor (SGGT) with high performance was developed. Friedreich's ataxia (FRDA) is a neurodegenerative disease where the first intron of the frataxin (FXN) gene exhibits an extended GAA repeat region. Herein, a SGGT biosensor was constructed based on G-quadruplex DNAzymes and graphene channels. The DNAzymes quantify the captured target DNA by producing a strong catalytic current signal depending on the peroxidase-like activity. The higher the target DNA quantity captured on the gate electrode is, the higher is the concentration of DNAzymes on the surface of the gate electrode, which generates a high catalytic current. Due to the excellent self-amplifying performance of the transistor, the current signal of the SGGT is several hundreds of times larger than in conventional electrochemistry under identical detection conditions. Moreover, a large current signal can be obtained in the case of a low concentration of H_2O_2 when compared to the case of an enzyme-catalyzed transistor. The SGGT biosensor also exhibits an ultra-low detection limit (32.25 fM), a wide linear range (100 fM–100 nM), and excellent selectivity. The results show that the SGGT biosensor has great potential in the early diagnosis of neurodegenerative diseases.

Received 31st January 2020,
Accepted 1st June 2020

DOI: 10.1039/d0an00205d

rsc.li/analyst

1. Introduction

Friedreich's ataxia (FRDA) is an autosomal recessive disorder and is the most common early-onset hereditary ataxia among Caucasians.[1] As other neurodegenerative diseases, such as myotonic dystrophy (CTG), fragile X syndrome (CGG),[2] Huntington's disease, and spinocerebellar ataxias (CAG),[3,4] the first intron of the frataxin (FXN) gene of FRDA exhibits an extended GAA repeat region.[5,6]Early diagnosis of this gene in neurodegenerative diseases is particularly important, especially in the early genetic screening of individuals. A number of molecular biology methods based on traditional sequencing technologies have been developed to analyse the trinucleotide repeats (TNRs).[7,8] These methods have high accuracy. However, they require the use of professional technologies and are time- and cost-demanding. Therefore, there is a broad market and a high demand for the development of rapid, simple, low-cost, and non-professional techniques. These methods are expected to be developed to fulfill the demands of modern medical diagnosis techniques and treatments. For instance, several fluorescence and electrochemical analysis methods have been reported.[9–11]

Graphene has been used in sensors for a long time: it exhibits a high electrical conductivity, excellent physical properties, mass-less carriers (both electrons and holes), high transparency (97.7% for single layers), and extremely high carrier mobility (10^5 cm^2 V^{-1} s^{-1}).[12,13] Stable single-layer graphene has been obtained *via* the physical exfoliation method by Novoselov *et al.* in 2004.[14,15] However, a large area of graphene could not be prepared. Recently, various methods, such as chemical vapor deposition (CVD),[16] electrochemical reduction,[17] and self-assembly of interfaces,[18] have started producing large and uniform sheets of graphene, and graphene devices have begun to advance by leaps and bounds. More importantly, the successful preparation of large-area and high-quality single-layer graphene *via* CVD has become a popular method.

Graphene transistors caught the attention of several research groups due to the excellent properties of graphene.[19] Contrary to the other sensors, solution-gated graphene transis-

[a]Ministry of Education Key Laboratory for the Synthesis and Application of Organic Functional Molecules, Hubei University, No. 368 Youyi Avenue, Wuchang, Wuhan 430062, China. E-mail: hehanping@hubu.edu.cn
[b]Ministry of Education Key Laboratory for the Green Preparation and Application of Functional Materials, Hubei Key Laboratory of Polymer Materials, Faculty of Materials Science and Engineering, Hubei University, No. 368 Youyi Avenue, Wuchang, Wuhan 430062, China

†Electronic supplementary information (ESI) available. See DOI: 10.1039/d0an00205d

tors (SGGTs) provide cost effectiveness, unique biocompatibility, ease of fabrication, significantly low operating voltage (below 1 V), and inherent signal amplification. A transistor-based biosensor is not only a sensor but also an amplifier.[20] Due to the inherent amplification of this device, small changes in its gate voltage result in a significant response of its channel current.[21] Conventional SGGTs often consist of a graphene channel, which is located between the source and the drain electrodes, and of an electrolyte situated between the graphene channel and the gate electrode.[22] In the solution-gated transistor, the classical direct dielectric material located between the channel and the gate electrode was replaced by an electrolyte solution, which acts as a dielectric layer. Consequently, SGGT devices are reusable and require only the replacement of the gate and of the electrolyte for their correct use. In addition, the channel current is closely related to the W/L (W and L are the width and length of the channel) of the channel and it can be scaled down to achieve its miniaturization. The current of the graphene active layer can be adjusted by varying its effective voltage, which is applied from the gate *via* the electrolyte. A weak electrochemical reaction at the gate electrode causes a change in the amplification factor of the effective gate voltage, which results in a significant response of the channel current.[23] Zheng's group has developed a SGGT-based sensor for glucose and uric acid detection[24] and for monitoring the lactic acid derived from the cancer cell metabolism with high sensitivity (300 nM).[25] In both works, the gates were modified and functionalized, and the devices showed a high performance. Li's group has reported a label-free nucleic acid sensor based on a SGGT with high sensitivity (1 fM).[26] However, the test sample requires a large dilution and the detection time is up to 2000 s.

The use of the SGGT device as a biosensor is based on the use of elements, such as enzymes, antibodies, and aptamers, which can undergo conductive chemical changes in the presence of specific molecules.[27–31] In this work, an ultrasensitive SGGT biosensor based on the DNAzyme catalysis was developed to detect the GAA TNR biomarker (Fig. 1). The G-rich R-DNA sequence combines with hemin to form a G-quadruplex conformation and exhibits a peroxidase-like activity.[32] Compared to most channel modification and capture, in the design the modification and capture of DNA would be performed at the gate, which would simplify the operation and reduce costs. The redox reaction occurs at the gate and changes the effective gate voltage, which causes a significant variation of the channel current. The redox reaction catalyzed by DNAzymes can reach equilibrium within 200 s. Moreover, the current change generated by the DNAzyme-catalysed H_2O_2 is significantly higher than the catalytic current generated when HRP is used as a signal in other transistors.[33] In this paper, the gate electrode is also used in a traditional electrochemistry experiment as the working electrode. The sensitivity of the transistor is significantly higher than that of the electrochemical method. The SGGT biosensor exhibits excellent selectivity and ultrasensitivity and ultra-low detection limits down to 32.25 fM with a small test volume (5 μL) in the biomarker trinucleotide repeat detection.

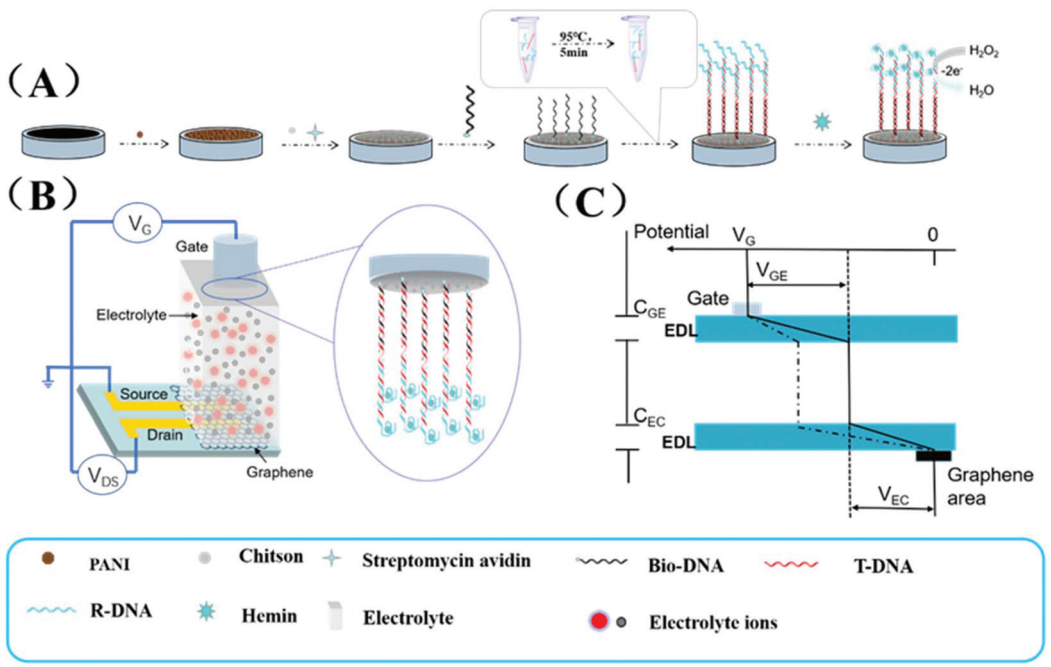

Fig. 1 (A) Gate modification process for the detection of GAA trinucleotide repeats. (B) Structure of the device including a graphene channel, functionalized gate, electrolyte, Au source and drain. (C) The potential drop between the gate and the channel of the SGGT modified with DNAzyme before (solid line) and after (dashed line) addition of H_2O_2 to the PBS solution.

2. Experimental

2.1 Materials and instrumentation

The aqueous solutions were prepared with ultrapure water (resistivity >18 MΩ cm) produced by using an Aquapro water purification system. H_2O_2 (30%) was purchased from Aladdin Industrial Co. (Shanghai, China) and PANI(Polyaniline) was purchased from Alfa Aesar Industrial Co. (Shanghai, China). A 20× phosphate buffered saline solution (PBS, pH 7.4) was purchased from Sangon Biotech Co., Ltd (Shanghai, China) and was diluted with water to 1× PBS for further use. $Fe(NO_3)_3{\cdot}9H_2O$, acetone, and absolute ethyl alcohol were obtained from Sinopharm Chemical Regent Co., Ltd. Polymethyl methacrylate (PMMA) was purchased from Shanghai Macklin Biochemical Co., Ltd and the single-layer graphene from Hefei Vigon Material Technology Co., Ltd. The rod-shaped glassy carbon electrodes (GCE) with a diameter of 3 mm were supplied by the Gaoss Union Instrument Company (Wuhan, China). The other reagents were of analytical grade and were used without further purification. The human serum samples used in the experiment were obtained from healthy adults (104 volunteers) from the Zijing Hospital (Wuhan, Hubei Province) and were diluted with PBS into a 10-fold-diluted solution for further use.

The acry/bis 40% solution (19 : 1), APS, TEMED, the DNA marker, and the oligonucleotides were purchased from Sangon Biotech Co., Ltd (Shanghai, China). The oligonucleotide sequence information is reported in the ESI.†

2.2 Characterization and experimental setup

A semiconductor parameter analyzer (2400S, Keithley Instruments Inc.) was employed to characterize the transistors. The glassy carbon electrodes (GCE) of 3 mm diameter were used either as the working electrodes or as gate electrodes. The electrochemical experiments were carried out on a CHI 660E electrochemical workstation (CH Ins., Shanghai, China), where a platinum wire was used as the counter electrode and a Ag/AgCl electrode and a saturated calomel electrode (SCE) were used as the reference ones. A patterned Au/Cr source and the drain electrodes were deposited onto the surface of a glass substrate *via* thermal evaporation (V22-300, KYKY Technology Co., Ltd). The morphology of the graphene was characterized *via* field-emission scanning electron microscopy (FE-SEM, JSM7100F, JEOL, Japan).

2.3 Fabrication of the SGGT based biosensors

The single-layer graphene was synthesized onto a series of copper foils *via* the CVD method and transferred onto the source and drain electrodes by using the wet transfer method.[33] The wet transfer process of the graphene is described in detail in the ESI.† Briefly, the graphene grows onto a copper sheet and PMMA is used to protect it during the transfer. Finally, the copper substrate is removed by immersing the sample in a $Fe(NO_3)_3$ solution and the protective layer is removed by immersing the sample in acetone solution. The area of the graphene in the channel measures 3 mm × 3 mm (Fig. S1†). The samples are then stored in a glove box for further use.

2.4 Modification of the gate electrodes

The GCEs were used as the gate electrodes for the SGGT. Initially, the treatment of the GCE is identical to the one reported in the previous section, and then, the electrodes were polished with an Al_2O_3 slurry for several minutes and sonicated with water and ethanol.[7] Successively, 5 μL of PANI (0.5 wt%) solution were added onto the GCE. Since PANI is a conductive polymer, its addition can improve the conductivity of the electrode. A quantity of 10 μL of streptavidin (SA) and chitosan (CHIT) mixture solution was dropped onto the PANI/GCE surface at room temperature for 1 h to form a membrane. Since CHIT exhibits efficient film forming properties, the SA can be modified on the electrode surface by mixing it with CHIT. A quantity of 10 μL of Bio-DNA (2 μM) was added onto the CHIT-SA/PANI/GCE gate electrode surface, resulting in the DNA immobilization on the gate due to the high affinity of biotin for SA. The gate electrode was rinsed with PBS after 0.5 h of incubation. The modified gate electrode (Bio-DNA/CHIT-SA/PANI/GCE) was labelled M-gate. A long DNA repeat easily formed its secondary structure. The hybridization reaction of a series of T-DNA samples with different concentrations and 5 μM R-DNA was heated up to 95 °C for 5 min and then, slowly cooled down to room temperature to ensure an adequate hybridization. A quantity of 10 μL of the hybridized mixture solution (T-DNA and R-DNA) was then dripped onto the M-gate and kept at 37 °C for 2 h. The sample was then rinsed with PBS. The R-DNA/T-DNA/M-gate was dipped into 50 μL of hemin (4 μM) solution for 1 h at room temperature to form the DNAzymes for the measurements.

2.5 Electrical measurements

The SGGT measurements were performed in a 1× PBS solution with the aid of a magnetic stirrer. The electrical performance and the sensing properties of the SGGT with different gate electrodes were investigated by using a 20 mL PBS (pH 7.4) solution and analysed by using a semiconductor parameter analyser. From the semiconductor parameter analyser, we can gain transfer curves (I_{DS} *versus* V_G) and time-dependent channel currents (I_{DS} *versus* time) of the device. The transfer curve was recorded at a fixed source–drain voltage (V_{DS} = 0.05 V) by varying gate voltages (V_G = 0 V–1 V) with a sweep rate of 0.01 V s^{-1}. According to the transfer curve of the device, the time-dependent channel currents were measured at a fixed V_G and V_{DS} (V_G = 0.6 V and V_{DS} = 0.05 V). After the time-dependent channel currents stabilized, H_2O_2 (final concentration, 10^{-5} M) was quickly added into the beaker.

A traditional three-electrode system was used to perform the experiments: a GCE, a Ag/AgCl electrode or a saturated calomel electrode (SCE) (saturated with KCl), and a Pt wire were used as the working, reference, and counter electrodes, respectively. Initially, electrochemical impedance spectroscopy (EIS) was carried out to study the electrochemical properties of the GCE layer at different modifications with a saturated

calomel electrode as the reference electrode. An EIS experiment, where 51 frequencies were sampled in the 100 kHz–100 mHz frequency range with 0.01 V amplitude, was conducted with a 0.5 mM $[Fe(CN)_6]^{3-/4-}$ redox probe in PBS. To measure the catalytic activity of the DNAzymes, an amperometric detection was performed at 0.6 V for 100 s to monitor the electrochemical reduction current after the redox reaction reached its steady state with a Ag/AgCl electrode as the reference electrode. The solution used consisted of a PBS buffer with 10^{-5} M H_2O_2.

3. Results and discussion

3.1 Design principle of the SGGT biosensor

Fig. 1 shows the structure of a SGGT biosensor with a graphene channel and a DNA-modified gate electrode. The area of the graphene measures 3 mm × 3 mm. The DNA-modified gate electrodes and the channel are connected *via* the electrolyte inside the device. Moreover, two interfaces in the device correspond to the interface between the gate/electrolyte (C_{GE}) and the electrolyte/graphene (C_{EC}). The gate voltage (V_G) is applied between the gate and the channel *via* the two interfaces and the electrolyte, as shown in Fig. 1. Furthermore, it is important that the device performance is only related to the two interfaces. The working mechanism of a SGGT biosensor is based on the catalysis of the H_2O_2 reaction *via* the modified DNAzymes on the gate. The resulting Faraday current affects the capacitance between the gate and the electrolyte (C_{GE}), and the change in C_{GE} further modifies the value of the effective gate voltage (V_G^{eff}). This affects eventually the current, which flows in the channel.[23]

The gate electrode modified with Bio-DNA on the GCE modified with SA/CHIT/PANI can be called M-gate (Bio-DNA/CHIT-SA/PANI/GCE). In the presence of T-DNA, R-DNA can hybridize and the R/T hybridization with the repeat DNA can occur. The R/T can be captured onto the surface of the M-gate since the Bio-DNA can hybridize with the end part of the repeat DNA. The R-DNA sequence is designed to have two functions: (1) to perform the hybridization with the repeat and (2) to form the G-quadruplex for the DNAzyme. The hemin/G-quadruplex DNAzyme gate electrode forms after the R-DNA/T-DNA/M-gate is incubated with hemin. The higher the number of target DNA sequences is, the higher is the quantity of R/T hybridization DNA segments captured onto the gate electrode surface. This generates an increase in the hemin/G-quadruplex DNAzyme present onto the gate electrode.

The DNAzyme can catalyse the electrochemical reaction of H_2O_2, which occurs onto the modified gate electrode surface. Moreover, this leads to an increase in the effective gate voltage (V_G^{eff}) and in the response of the channel current (I_{DS}). Such response of the channel current in the SGGT due to the applied V_G varies based on the concentration of DNAzymes on the gate electrode in the sensing application. The amount of DNAzymes on the gate electrode can be defined *via* the H_2O_2 reaction.

The I_{DS} value of the SGGT biosensor with a fixed V_G and V_{DS} is given by eqn (1).[34] The redox current on the gate, which is generated by the electrochemical reaction of H_2O_2, generates a decrease in the potential drop, which induces an increase in V_G^{eff}. The variation of V_G^{eff} may result in a change of the channel current. The V_G^{eff} value of the SGGT biosensor increases with the amount of DNAzymes. This quantity is proportional to the T-DNA concentration and is given by eqn (2).[19,35] To summarize, the channel current is closely related to the amount of DNAzymes, as reported in eqn (3). The specific parameters and the calculation formulas are listed in the ESI.†

$$I_{DS} = \frac{q\mu p_0 tW}{LV_P}\left(V_P - V_G^{eff} + \frac{V_{DS}}{2}\right)V_{DS} \quad \left(\text{when } |V_{DS}| \ll \left|V_P - V_G^{eff}\right|\right) \tag{1}$$

$$V_G^{eff} = 2.30(1+\gamma)\frac{kT}{2q}\log\left[W_{DNAzyme}\right] + C_2 \tag{2}$$

$$I_{DS} \propto \alpha \log[W_{DNAzyme}] + \text{constant} \tag{3}$$

The operating mechanism of the SGGT biosensor can be further explained by the real-time I_{DS} response curve with a GCE as the gate electrode. In the presence of T-DNA, the channel current of the SGGT increases significantly due to the change in the V_G^{eff} value upon the addition of 10^{-5} M H_2O_2, as shown in Fig. 2. However, the DNAzyme cannot be formed when no T-DNA, R-DNA, or hemin is present independently from the applied current (curves b, c, and d in Fig. 2). These results indicate that the SGGT biosensor is very effective and can be used in the detection of repeat DNA. We also studied the effect of H_2O_2 on the device as shown in Fig. S2.† When the Ag/AgCl electrode was used as the gate electrode, the channel current showed a small reduction of 1 μA after adding 10^{-5} M H_2O_2 to the electrolyte. We speculate that this may be due to H_2O_2 oxidizing the graphene channel and p-type doping the graphene.

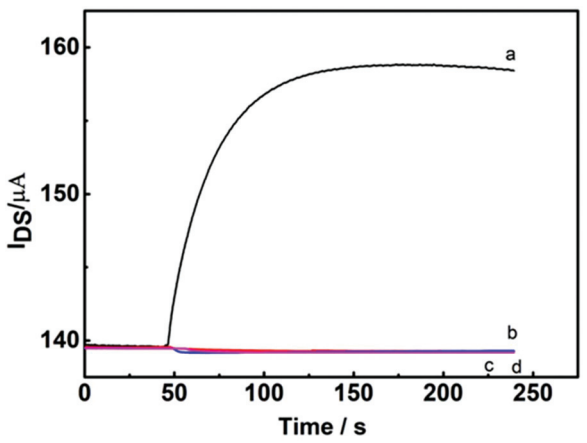

Fig. 2 The I_{DS} response after adding 10^{-5} M H_2O_2 of (a) hemin/R-DNA T-DNA/M-gate; (b) hemin/R-DNA/m-gate; (c) R-DNA/T-DNA/m-gate and (d) hemin/T-DNA/m-gate (T-DNA = 10 pM).

3.2 Preparation and characterization of the SGGT biosensor

The transfer procedure of graphene is a very important step because it greatly affects the performance of the SGGT biosensor. A uniform and smooth graphene interface, in fact, improves the output signal. The detailed transfer process is in the ESI.† Fig. 3A shows a typical optical image of a graphene film, in which the material was transferred onto the substrate. The wrinkles may be caused in the cooling stage because of the difference in the thermal expansion coefficients between the copper foil and the graphene film. In addition, some impurities (white spots) were observed in the SEM image, and these impurities were most likely PMMA residues generated by the transfer process. If the graphene breaks during the transfer procedure, the channel current is unstable and it is difficult to reach the plateau when compared to a uniform graphene layer, as shown in Fig. S3.†

The DNA hybridization is also a very significant process in the formation of the DNAzyme. Initially, this was analysed *via* native PAGE. More details about this experimental process can be found in the ESI.† As shown in Fig. 3B, the lanes b, c, and d show the bands of bio-DNA, T-DNA, and R-DNA, respectively. If no repeat DNA is present, the bio-DNA cannot hybridize with the R-DNA and no new bands can be observed in lane e. In the presence of T-DNA, R-DNA can hybridize multiple times with the repeat DNA. Moreover, the bio-DNA can bind to the partial sequence of the 3′ end in the repeat DNA. Consequently, the duplex DNA is formed. As shown in lane f, the original bio-DNA, R-DNA, and T-DNA disappear, and a new band appears. These results indicate that the bio/R/T-DNA hybridization complex can form effectively only in the presence of T-DNA, and that the R/T DNA complex can be captured by the bio-DNA-modified gate.

In order to further evaluate the stepwise fabrication of the electrodes, the preparation process of the DNA-modified gate electrodes was characterized *via* a series of conventional electrochemical methods, such as EIS, in which the modified gate was used as the working electrode. As shown in Fig. S4A,† the electron-transfer resistance (R_{et}) of the bare GCE is rather small (50 Ω), when $[Fe(CN)_6]^{3-}/[Fe(CN)_6]^{4-}$ is used as the redox probe. Moreover, PANI was used to improve the conductivity of the gate electrodes. As shown in Fig. S4B,† the gate electrode with PANI shows a smaller impedance than the electrode without PANI: this observation proves that PANI can significantly enhance the conductivity of the system. The value of R_{et} increases to 297 Ω and 428 Ω (Fig. S4A†) respectively after the modification of the gate electrode with CHIT/SA/PANI and Bio-DNA. When the hybridized complexes (R/T DNA) are captured onto the modified GCE, the value of R_{et} increases significantly from 428 Ω to 525 Ω. During the layer-by-layer assembly process of DNA, the impedance of the electrode shows a gradual increase. These results further indicate the successful hybridization of R-DNA and T-DNA and the capture of the hybridized complexes.

A change at the gate/electrolyte (C_{GE}) interface results in a variation in the effective gate voltage (V_G^{eff}) and in the response of the channel current. The bipolar properties of graphene can be observed on the SGGT by using a transfer characteristic curve, which shows the relationship between I_{DS} and V_G at V_{DS} = 0.05 V. According to the transfer curve of the SGGT in Fig. 4, the SA/CHIT/PANI film on the gate electrode generates a huge left shift (280 mV) in PBS (pH = 7.4) due to the intrinsic positive charge of CHIT. After the immobilization of the Bio-DNA and the hybridization of the R/T DNA complexes onto the gate, two clear horizontal right shifts of 50 mV and 120 mV, respectively, can be observed. The inherent DNA charges produce a surface dipole and, for this reason, the work function of the gate is lower after the DNA is captured onto the gate.[36] The change in the transfer curve may be attributed to the variation of V_{offset} in eqn (4). The specific parameters and calculation formulas are reported in detail in the ESI.†

$$\Delta V_{offset} = \frac{nQ_{DNA}}{\varepsilon_t \varepsilon_0} t_{DNA} \quad (4)$$

Therefore, the surface potential of the gate electrode lowers due to the introduction of the negative charges of the DNA molecule following the modification of the electrode surface.

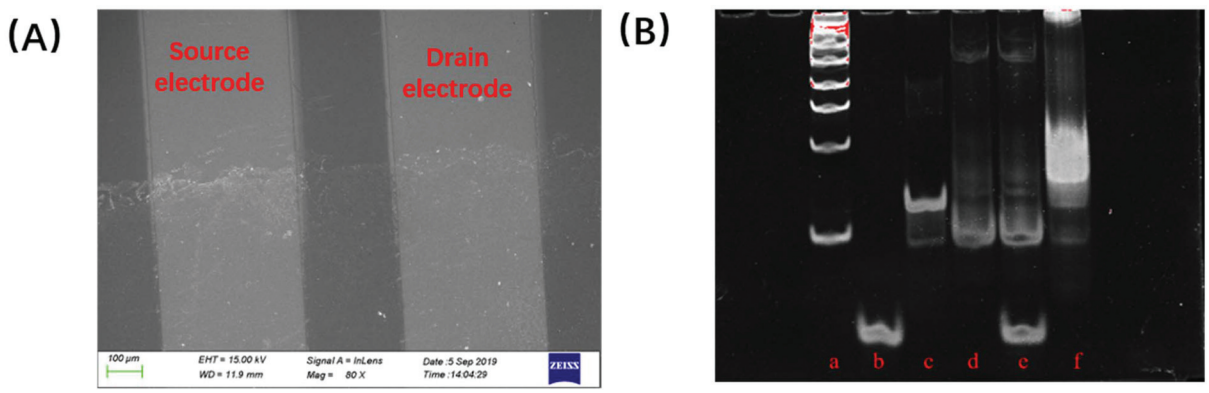

Fig. 3 (A) SEM images of the transferred graphene, (B) the 15% native PAGE analysis: lane a, DNA marker ladder; lane b, Bio-DNA; lane c, T-DNA; lane d, Rep-DNA; lane e, Bio-DNA + R-DNA; lane f, Bio-DNA + T-DNA + R-DNA. The DNA concentration was 10 µM. Voltage: 120 V; time: 1 h.

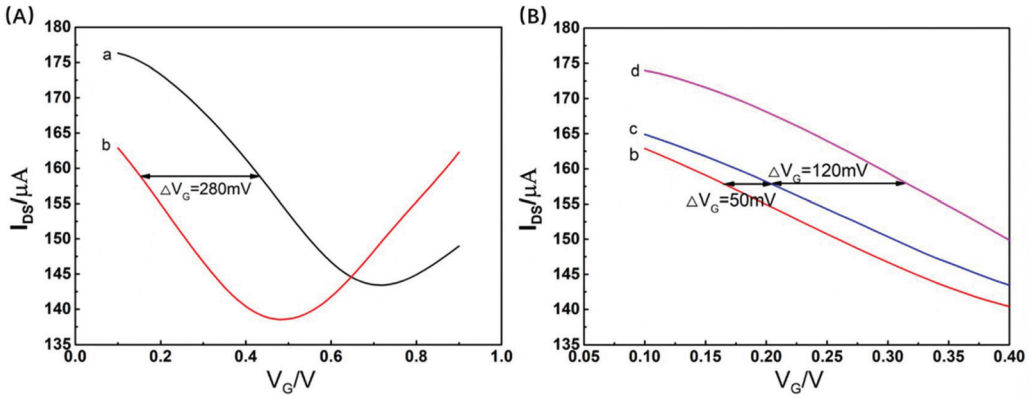

Fig. 4 (A) Transfer characteristics (I_{DS} *vs.* V_G) of the SGGT biosensor measured in PBS solution (7.4) with a modified gate electrode. (a) The bare GCE, (b) the CHIT-SA/PANI modified gate; (B) the horizontal shifts of the transfer curves after the immobilization of Bio-DNA (c) and the hybridization of T-DNA/Rep-DNA (d) on gate electrodes. V_{DS} = 0.05 V.

The DNA hybridization introduces more negative charges stepwise, and this results in a right shift of the transfer curve.

3.3 Optimization of measurement conditions

In the application of the SGGT biosensor, the amount of Bio-DNA, the incubation time, and the buffer pH are important parameters, which have a significant effect on the biosensor. In this experiment, sufficient Bio-DNA is required to capture the T-DNA in a wide range. Therefore, the binding time of the Bio-DNA/SA pair on the gate has been optimized. As shown in Fig. 5A, the change in I_{DS} reaches a plateau after 30 min of incubation. This implies that 30 minutes is the optimal time for the system in the presence of a high enough concentration of Bio-DNA (10 μL, 2 μM). Since the DNA detection was achieved *via* the catalysis reaction of H_2O_2 by the DNAzyme on the gate, the amount of the DNAzyme is pivotal for the SGGT biosensor. Here, the optimal incubation time value is investigated to achieve a high detection accuracy when the Bio-DNA-M-gate captures the target. The channel current gradually increases from 3 μA to 24 μA upon the increase of the incubation time due to the DNAzyme-catalysed reaction (Fig. 5B). Therefore, a time of 2 h was selected as the optimal condition for the Bio-DNA to T-DNA hybridization. In addition, the pH value of the buffer significantly affects the detection efficiency of the SGGT biosensor. As shown in Fig. 5C, the channel current is rather low under acidic conditions, but it reaches its maximum for a biological pH of the buffer. A buffer solution with pH 7 was then employed in the experiments.

3.4 Detection of target DNA

Initially, channel current responses were investigated with the different concentrations of targets for the SGGT biosensor. The channel current response can be measured more conveniently when the transistor biosensor is used with fixed gate and drain voltages. The channel current response of the device was measured after the addition of H_2O_2, and the hemin/R-DNA/T-DNA/M-gate was used as the gate electrode (Fig. 6A). Upon an increase in the concentration of the target DNA, the amount of the DNAzyme on the gate surface increases, which results in a higher channel current due to the H_2O_2 catalysis. As shown in Fig. 6A, the intensity of the channel current increases gradually with the increase in the T-DNA concentration. This indicates

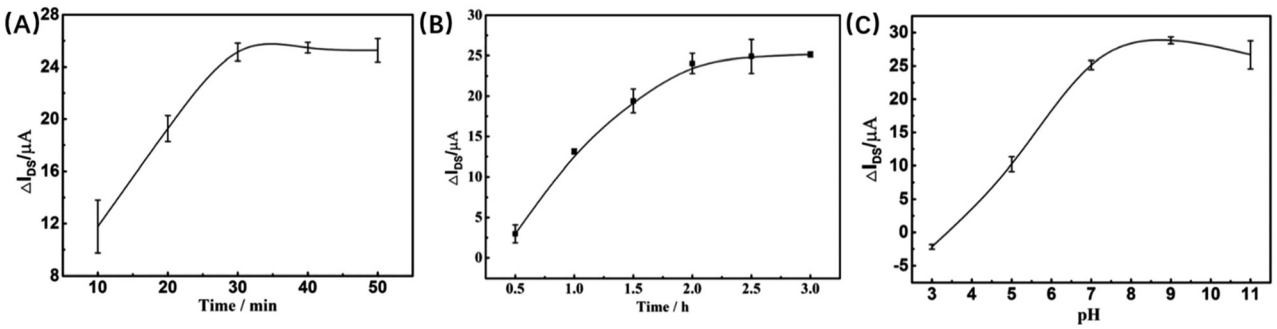

Fig. 5 The channel current responses of the devices to the addition of H_2O_2 at the operational voltages of V_G = 0.6 V and V_{DS} = 0.05 V. (A) The effect of the binding time between Bio-DNA and SA on the gate for the SGGT biosensor. (B) The effect of the incubation time for the SGGT biosensor when the Bio-DNA-modified gate captures R/T-DNA. (C) The effect of buffer pH. The target DNA concentration was 100 pM. The number of test samples for each set of data is 3.

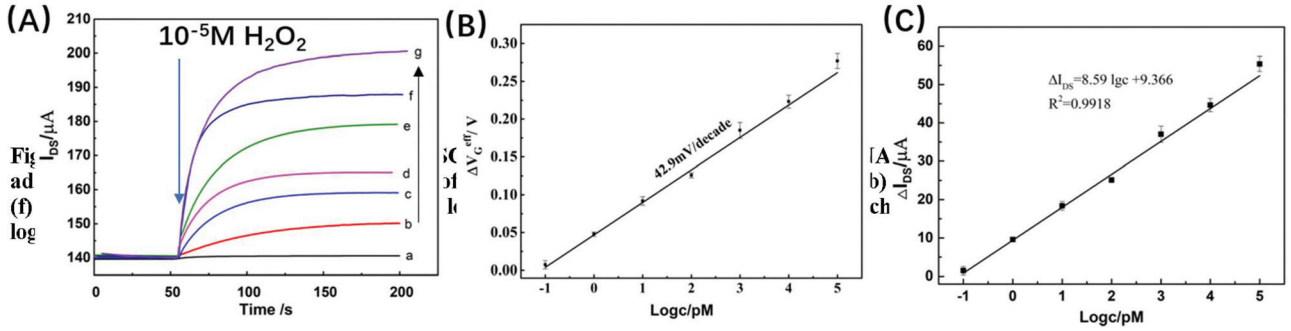

Fig. 6 (A) The channel current responses of the SGGT-based DNAzyme biosensor with R-DNA/T-DNA/m-gate as the gate electrode to the addition of H_2O_2 at the operational voltages of V_G = 0.6 V and V_{DS} = 0.05 V. (a) 0.1 pM; (b) 1 pM; (C) 10 pM; (d) 100 pM; (e) 1 nM; (f) 10 nM; (g) 100 nM. (B) Plot of ΔV_G^{eff} *vs.* log *c*/pM. (C) A linear relationship between the channel current response and target DNA logarithmic concentration.

that the electrochemical activity, which takes place onto the gate electrode, is solely dependent on the T-DNA concentration. According to the channel current, the effective gate voltage can be calculated by the transconductance through the transfer curve.[24,33,37,38] We analysed the relationship of the change of effective gate voltage and the target concentration (Fig. 6B), and found that there is an excellent linearity $\Delta V_G^{eff} = 0.0429 \log C + 0.0468$. The data also show that the slope of ΔV_G^{eff} to the logarithm of the target concentration is 42.9 mV per decade. According to previous reports,[39–42] there is also a relationship between the response of the channel current and the target concentration. Moreover, the relationship between channel current variations and target concentrations was also studied. An excellent linear relationship was found with the equation $\Delta I_{DS} = 8.59 \log c + 9.37$ (R^2 = 0.9918) over a wide concentration range (100 fM–100 nM) (Fig. 6C). These results indicated that eqn (3) was reasonable in some concentration ranges, and the variations of channel currents have some linearity with the concentrations of the target on the gate.

The changes in the gate current were less than 3 nA only (Fig. S5†), whereas the channel current response reaches 57 μA, when the target DNA concentration increases from 0.1 pM to 100 nM. The data show that the channel current is several orders of magnitude higher than the gate current. In comparison, the sensing properties of the DNAzyme-modified gate electrode used as the working electrode were investigated *via* a traditional electrochemical platform. When the DNA concentrations are 10 nM and 100 nM, the current measures 0.09 μA and 0.13 μA, respectively (Fig. 7A). Surprisingly, the current in the channel is 44.6 μA and 55.4 μA, respectively. Normally, the limit of detection (LOD) is defined when the signal-to-noise ratio measures 3. In this case, the signal-to-noise ratios are 2.24 and 3.25 for a traditional three-electrode system when the concentration of T-DNA is 10 nM and 100 nM, respectively. This indicates that the detection limit measures only 100 nM (Fig. S6†). Compared with traditional electrochemical methods, the SGGT exhibits a relatively large current signal and a large signal-to-noise ratio (Fig. 7B). The detection limit measures 32.25 fM for a SGGT biosensor. These results demonstrate that the SGGT biosensors exhibit

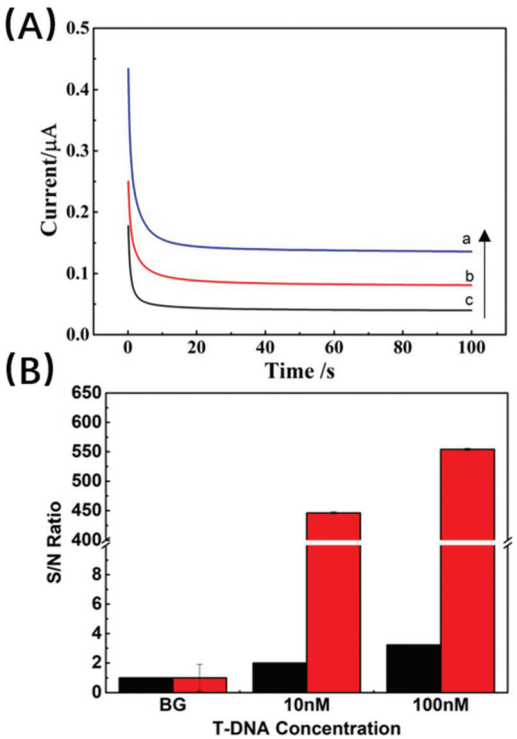

Fig. 7 (A) Traditional electrochemical current responses from the DNAzyme catalysed redox that was incubated in different T-DNA concentrations. (a) 100 nM; (b) 10 nM; (c) 0. (B) Comparison of signal-to-noise ratio between traditional electrochemistry and the SGGT biosensor at different T-DNA concentrations. The number of test samples for each set of data is 3.

advantages such as signal amplification and high sensitivity. When compared to other detection methods for the detection of nucleic acids (Table 1), the combination of DNAzymes and SGGTs shows a good detection limit and a wide linear range without the application of any external amplification method.

3.5 Selectivities, reproducibility and stability of the SGGT

Another important characteristic of a biosensor is its selectivity. A series of interfering TNRs, such as CCG, CTG, ATT,

Table 1 Comparison of different methods for nucleic acid detection

Detection method	Target	Linear range	LOD	Ref.
Fluorescence	CGG TNR	0 to 150 nM	84 pM	43
Electrochemistry	CAG TNR	100 pM to 1 μM	24 pM	7
Electrochemistry	CAG TNR	1 pM to 100 nM	0.15 pM	11
SGGT	Random sequence	1 fM to 10 pM	1 fM	26
SGGT	GAA TNR	100 fM to 100 nM	32.25 fM	This work

TGG, CAG, and CGG, in a concentration of 10 pM were used in the experiments. These sequences are related to neurodegenerative diseases. The other conditions were left unchanged from the previous experiments, except that the GAA TNR was replaced by a different TNR. Here, the concentrations of interfering repeats are 10 times that of the target in order to verify the selectivity better. The channel current responses were measured for these different TNA (Fig. 8A), which showed that the current of the target GAA was much higher than that of interfering repeats obviously. According to the channel current, the effective gate voltages by the reaction of H_2O_2 were also calculated. The inset in Fig. 8B shows the ΔV_G^{eff} of the biosensor detected from different TNP, which indicates that the change with the GAA target is about 20 times higher than that of the case with interfering TNP. Fig. 8B shows the variations of channel currents (ΔI_{DS}) of the biosensor, which is comparable with ΔV_G^{eff}. This result clearly demonstrates the high selectivity of the SGGT biosensors for T-DNA in the TNR biomarkers of neurodegenerative diseases.

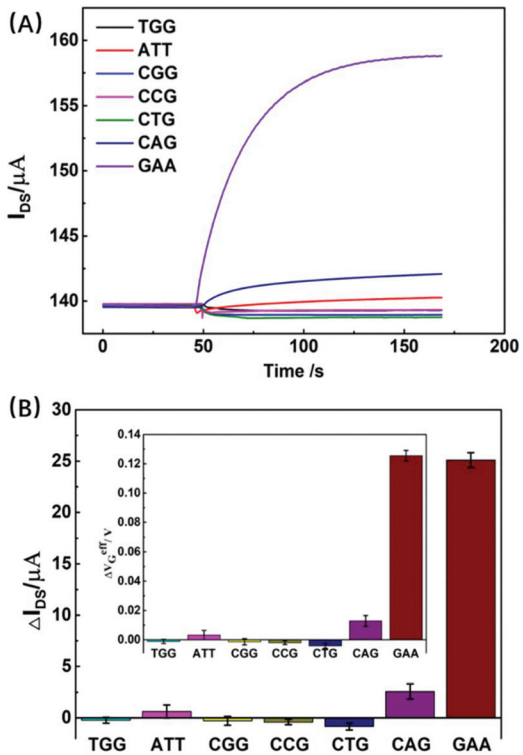

Fig. 8 (A) The channel current response of the SGGT-based biosensor with the interfering trinucleotide repeats and GAA trinucleotide repeats. (B) ΔI_{DS} response of the interfering trinucleotide repeats and GAA trinucleotide repeats. The inset image displays the calculated ΔV_G^{eff} response to interfering trinucleotide repeats and GAA trinucleotide repeats. The number of test samples for each set of data is 3.

Moreover, the reproducibility of this sensor, which is important for its future practical application, is shown in Fig. S7.† The same concentration (10 pM) of the GAA TNR was tested using the seven modified gate electrodes under identical experimental conditions. The results show that the seven sets of gate electrodes exhibit a good reproducibility with an RSD value of approximately 0.08%. Since the dielectric layer of this sensor consists of a buffer, the stability of the device is critical. To test this parameter under working conditions, several gate electrodes were obtained and these devices were completely immersed in the buffer. Fig. S8A† shows that the charge neutrality point (CNP) of the transfer curves slightly shifts for up to 10 h. The transfer curves of the device were measured every two hours and the results show that the CNP of the transfer curve barely moves. Furthermore, the stability of the device in the short-term was monitored based on the transfer curve data. In the short-term test, the CNP of the transfer curves was continuously monitored from 0 to 100 times. The transfer curves during this period maintain an excellent stability when the tests are repeated 100 times (Fig. S8B†). The results of the long-term test are similar to the short-term ones. The stability tests show that the device exhibits a good stability in both long- and short-term.

3.6 Real sample detection

To explore the applicability of the SGGT biosensors in a real sample, a series of T-DNA samples in serum were used to show the detection limit of the device. In the actual sample test, a 10-fold dilution of human serum was used to separate the target GAA TNR into samples with different concentrations (1 pM, 10 pM, and 100 pM). The other conditions were left unchanged, except that the GAA TNR diluted with serum was used instead of the original GAA TNR. Table 2 presents the data obtained from this experiment: the method used is quite accurate. The recovery varies in the 91.00%–102.5% range with a relative standard deviation between 2.4% and 0.17%. These results show that the SGGT biosensors can be used for the trinucleotide repeat detection in real biological environments. This indicates that this novel biosensor constitutes a potential tool for the early diagnosis of neurodegenerative diseases.

Table 2 Detection of GAA trinucleotide repeats in human serum (n = 3) with the proposed biosensor

Sample	Added (pM)	Found (pM)	Recovery (%)	RSD (%)
1	1.00	0.990	99.00	2.4
2	10.0	9.100	91.00	1.5
3	100	102.5	102.5	0.17

4. Conclusion

In summary, a SGGT was successfully designed and used to detect the trinucleotide repeat GAA biomarker. The device shows a high sensitivity and an excellent selectivity. In this work, a sandwiched-DNA structure was used to detect T-DNA, which hybridizes with bio-DNA on the gate, and R-DNA multiplies. The G-quadruplex in the R-DNA is captured onto the gate and forms DNAzymes in the presence of hemin. Successively, H_2O_2 is added to trigger the redox reaction. The number of electrons transferred during the redox reaction is proportional to the amount of R-DNA, which is proportional to the amount of T-DNA. The SGGT shows a current response 400 times higher than in the case of a traditional electrochemical response. The variations of effective gate voltage and the channel currents linearly increase upon the increase of the T-DNA. The mathematical expressions of the current response are $\Delta V_G^{eff} = 0.0429 \log c + 0.0468$ and $\Delta I_{DS} = 8.59 \log c + 9.37$ ($R^2 = 0.9918$) respectively. They are valid over a wide range of concentrations (100 fM–100 nM) with an ultra-low LOD of 32.25 fM. Moreover, this device was successfully used to detect the biomarker in biological environments. This method shows great promise to develop an early-diagnosis method for neurodegenerative diseases. In addition, the results of this work indicate that the SGGT is an excellent platform to manufacture highly sensitive and simple biosensors.

Ethical statement

All experiments were performed in accordance with the relevant laws and institutional guidelines from the Zijing Hospital (Wuhan, China) and "Regulations on the administration of medical institutions" Guidelines from China, and approved by the ethics committee at Hubei University. All experiments were performed in compliance with the laws of the People's Republic of China. Informed consents were obtained from the human participants of this study.

Conflicts of interest

There are no conflicts to declare.

Acknowledgements

This work was financially supported by the National Natural Science Foundation of China (No. 21575035 and 51672074).

References

1 A. Collins, Clinical neurogenetics: Friedreich ataxia, *Neurol. Clin.*, 2013, **31**(4), 1095–1120.
2 Y. H. Fu, D. P. Kuhl, A. A. Pizzuti, M. Pieretti, J. S. Sutcliffe, S. Richards, A. J. Verkerk, J. J. Holden, R. G. Fenwick and S. T. Warren, Variation of the CGG repeat at the fragile x site results in genetic instability: resolution of the sherman paradox, *Cell*, 1991, **67**, 1047.
3 R. H. Myers, M. E. MacDonald, W. J. Koroshetz, M. P. Duyao, C. M. Ambrose, S. A. Taylor, M. Barnes, G. J. Srinidhi, C. S. Lin, W. L. Whaley, A. Lazzerini, M. M. Schwarz, G. Wolff, E. D. Brid, J. P. Vonsattel and J. F. Gusella, De novo expansion of a(CAG)n repeat in sporadic Huntington's disease, *Nature*, 1993, **5**, 168–173.
4 S. M. Mirkin, Expandable DNA Repeats and Human Disease, *Nature*, 2007, **447**, 932–940.
5 G. S. Chandok, M. P. Patel, S. M. Mirkin and M. M. Krasilnikova, Effects of Friedreich's ataxia GAA repeats on DNA replication in mammalian cells, *Nucleic Acids Res.*, 2012, **40**(9), 3964–3974.
6 V. Campuzano, L. Montermini, M. D. Molto, L. Pianese, M. Cossee, F. Cavalcanti and M. Pandolfo, Friedreich's Ataxia: Autosomal Recessive Disease Caused by an Intronic GAA Triplet Repeat Expansion, *Science*, 1996, **271**(5254), 1423–1427.
7 Y. L. Liu, J. Li, G. Chang, R. Z. Zhu and H. P. He, A novel electrochemical method based on screen-printed electrodes and magnetic beads for detection of trinucleotide repeat sequence d(CAG)n, *New J. Chem.*, 2018, **42**(12), 9757–9763.
8 H. P. He, X. Q. Peng, M. Huang, G. Chang, X. H. Zhang and S. F. Wang, An electrochemical impedance sensor based on a small molecule modified Au electrode for the recognition of a trinucleotide repeat, *Analyst*, 2014, **139**(21), 5482–5487.
9 B. H. Le, H. N. Joo, D. W. Hwang, K. W. Kim and Y. J. Seo, AuNP-CTG based probing system targeting CAG repeat DNA and RNA sequences, *Bioorg. Med. Chem. Lett.*, 2017, **27**(16), 3772–3775.
10 T. Shibata and K. Nakatani, Bicyclic and tricyclic C-C mismatch-binding ligands bind to CCG trinucleotide repeat DNAs, *ChemBioChem*, 2018, **54**(51), 7074–7077.
11 J. Li, Y. L. Liu, X. Q. Zhu, G. Chang, H. P. He, X. H. Zhang and S. F. Wang, A Novel Electrochemical Sensor Based on a Double-Signal Technique for d(CAG)n Trinucleotide Repeats, *ACS Appl. Mater. Interfaces*, 2017, **9**(50), 44231–44240.
12 T. D. Thanh, J. Balamurugan, S. H. Lee, N. H. Kim and J. H. Lee, Effective seed-assisted synthesis of gold nanoparticles anchored nitrogen-doped graphene for electrochemical detection of glucose and dopamine, *Biosens. Bioelectron.*, 2016, **81**, 259–267.
13 C. I. L. Justino, A. R. Gomes, A. C. Freitas, A. C. Duarte and T. A. P. Rocha-Santos, Graphene based sensors and sensors, *TrAC, Trends Anal. Chem.*, 2017, **91**, 53–66.
14 A. K. Geim, Random walk to graphene (nobel lecture), *Angew. Chem., Int Ed*, 2011, **50**(31), 6966–6985.
15 K. S. Novoselov, A. K. Geim, S. V. Morozov, D. Jiang, Y. Zhang, S. V. Dubonos, I. V. Grigorieval and A. A. Firsov, Electric field effect in atomically thin carbon films, *Science*, 2004, **306**(5696), 666–669.

16 C. Xie, P. Lv, B. Nie, J. S. Jie, X. W. Zhang, Z. Wang, P. Jiang, Z. Z. Hu, L. B. Luo, L. B. Zhu, Z. F. Zhu, L. Wang and C. Y. Wu, Monolayer graphene film/silicon nanowire array Schottky junction solar cells, *Appl. Phys. Lett.*, 2011, **99**(13), 133113.

17 L. Shi, Y. Li, X. Rong, Y. Wang and S. Ding, Facile fabrication of a novel 3D graphene framework/Bi nanoparticle film for ultrasensitive electrochemical assays of heavy metal ions, *Anal. Chim. Acta*, 2017, **968**, 21–29.

18 L. Shi, Z. Chu, Y. Liu, W. Jin and N. Xu, In Situ Fabrication of Three-Dimensional Graphene Films on Gold Substrates with Controllable Pore Structures for High-Performance Electrochemical Sensing, *Adv. Funct. Mater.*, 2014, **24**(44), 7032–7041.

19 F. Yan, M. Zhang and J. H. Li, Solution-gated graphene transistors for chemical and biological sensors, *Adv. Healthcare Mater.*, 2014, **3**(3), 313–331.

20 N. Wang, A. Yang, Y. Fu, Y. Li and F. Yan, Functionalized organic thin film transistors for biosensing, *Acc. Chem. Res.*, 2018, **52**(2), 277–287.

21 F. Yan and H. Tang, Editorial: application of thin-film transistors in label-free DNA sensors, *Expert Rev. Mol. Diagn.*, 2010, **10**(5), 547–549.

22 P. Lin and F. Yan, Organic thin-film transistors for chemical and biological sensing, *Adv. Mater.*, 2012, **24**(1), 34–51.

23 M. Zhang, C. Liao, C. H. Mak, P. You, C. L. Mak and F. Yan, Highly sensitive glucose sensors based on enzyme-modified whole-graphene solution-gated transistors, *Sci. Rep.*, 2015, **5**, 8311.

24 C. Xiong, T. F. Zhang, W. Y. Kong, Z. X. Zhang, H. Qu, W. Chen, Y. B. Wang, L. B. Luo and L. Zheng, ZIF-67 derived porous Co3O4 hollow nanopolyhedron functionalized solution-gated graphene transistors for simultaneous detection of glucose and uric acid in tears, *Biosens. Bioelectron.*, 2018, **101**, 21–28.

25 L. B. Yu, Y. Li, M. Yu, W. Lu, Q. Hao, L. Jian and Z. Lei, Porous carbon supported nanoceria derived from one step in situ pyrolysis of Jerusalem artichoke stalk for functionalization of solution-gated graphene transistors for real-time detection of lactic acid from cancer cell metabolism, *Biosens. Bioelectron.*, 2019, **140**, 111271.

26 S. S. Li, K. Huang, Q. Fan, S. Yang, T. Shen, T. Mei, Y. Y. Wang, X. B. Wang, G. Chang and J. H. Li, Highly sensitive solution-gated graphene transistors for label-free DNA detection, *Biosens. Bioelectron.*, 2019, **136**, 91–96.

27 R. X. He, M. Zhang, F. Tan, P. H. Leung, X. Z. Zhao, H. L. Chan, W. Yang and F. Yan, Detection of bacteria with organic electrochemical transistors, *J. Mater. Chem.*, 2012, **22**(41), 22072.

28 L. D. Kergoat, B. Piro, D. T. Simon, M. C. Pham, V. NoeL and M. Berggren, Detection of glutamate and acetylcholine with organic electrochemical transistors based on conducting polymer/platinum nanoparticle composites, *Adv. Mater.*, 2014, **26**(32), 5658–5664.

29 D. Khodagholy, J. Rivnay, M. Sessolo, M. Gurfinkel, P. Leleux, L. H. Jimison, E. Stavrinidou, T. Herve, S. Sanaur, R. O. Owens and G. G. Malliaras, High transconductance organic electrochemical transistors, *Nat. Commun.*, 2013, **4**, 2133.

30 Z. T. Zhu, J. T. Mabeck, C. C. Zhu, N. C. Cady, C. A. Batt and G. G. Malliaras, A simple poly (3,4-ethylene dioxythiophene)/poly (styrene sulfonic acid) transistor for glucose sensing at neutral pH, *Chem. Commun.*, 2004, **13**(13), 1556–1557.

31 S. Y. Yang, J. A. Defranco, Y. A. Sylvester, T. J. Gobert, D. J. Macaya, M. O. Róisín and G. G. Malliaras, Integration of a surface-directed microfluidic system with an organic electrochemical transistor array for multi-analyte sensors, *Lab Chip*, 2009, **9**(5), 704–708.

32 P. Travascio, A. J. Bennet, D. Y. Wang and D. Sen, A ribozyme and a catalytic DNA with peroxidase activity: active sites versus cofactor-binding sites, *Chem. Biol.*, 1999, **6**(11), 779–787.

33 F. Ying, X. W. Nai, Y. Anneng, K. L. Helen, L. Li and F. Yan, Highly Sensitive Detection of Protein Biomarkers with Organic Electrochemical Transistors, *Adv. Mater.*, 2017, 1703787.

34 C. Z. Liao, C. H. Mak, M. Zhang, H. L. Chan and F. Yan, Flexible organic electrochemical transistors for highly selective enzyme sensors and used for saliva testing, *Adv. Mater.*, 2014, **27**(4), 676–681.

35 Z. Meng, Z. L. Cai, L. Y. Yan, K. L. Zhi, F. G. Feng and F. Yan, High-Performance Dopamine Sensors Based on Whole-Graphene Solution-Gated Transistors, *Adv. Funct. Mater.*, 2014, **24**, 978–985.

36 P. Lin, X. Luo, I. M. Hsing and F. Yan, Organic electrochemical transistors integrated in flexible microfluidic systems and used for label-free DNA sensing, *Adv. Mater.*, 2011, **23**(35), 4035–4040.

37 P. Lin, X. Luo, I. M. Hsing and F. Yan, Organic electrochemical transistors integrated in flexible microfluidic systems and used for label-free DNA sensing, *Adv. Mater.*, 2011, **23**(35), 4035–4040.

38 R. R. Wang, Y. Mao, H. Qu, W. Chen, A. J. Ma and L. Zheng, Highly sensitive and selective sulfite sensors based on solution-gated graphene transistors with multi-walled carbon nanotube functionalized gate electrodes, *Food Chem.*, 2019, 101–106.

39 Q. Fan, J. H. Li, Y. H. Zhu, Z. L. Yang, T. Shen, Y. Z. Guo, L. H. Wang, T. Mei, J. Y. Wang and X. B. Wang, Functional Carbon Quantum Dots for Highly Sensitive Graphene Transistors for Cu^{2+} Ion Detection, *ACS Appl. Mater. Interfaces*, 2020, **12**(4), 4797–4803.

40 M. Ma, Y. Zhou, J. Li, Z. Ge, H. He, T. Tao, Z. Cai, X. Wang, G. Chang and Y. He, Non-invasive detection of glucose via a solution-gated graphene transistor, *Analyst*, 2020, **145**(3), 887–896.

41 G. E. Fenoy, W. A. Marmisolle, O. Azzaroni and W. Knoll, Acetylcholine biosensor based on the electrochemical functionalization of graphene field-effect transistors, *Biosens. Bioelectron.*, 2020, **148**, 111796.

42 L. J. Zhang, Z. Liu, C. Xiong, L. Zheng, Y. S. Ding, H. B. Lu, G. B. Zhang and L. Z. Qiu, Selective recognition of Histidine enantiomers using novel molecularly imprinted organic transistor sensor, *Org. Electron.*, 2018, 254–260.

43 Z. Q. Ren, X. Q. Zhu, H. H. Lv, H. Liu, H. P. He, X. H. Zhang and S. F. Wang, A fluorescent method based on magnetic nanoparticles for detection of CGG trinucleotide repeat genes, *New J. Chem.*, 2019, **43**, 1322.